Circulating exosomes from patients with peripheral artery disease influence vascular cell migration and contain distinct microRNA cargo

Thomas A. Sorrentino, MD[a], **Phat Duong, BS**[b], **Laura Bouchareychas, PhD**[b], **Mian Chen, MD**[a], **Allen Chung, BS**[b], **Melinda S. Schaller, MD**[a], **Adam Oskowitz, MD, PhD**[a], **Robert L. Raffai, PhD**[a,b], **Michael S. Conte, MD**[a]

[a]Department of Vascular and Endovascular Surgery, University of California

[b]San Francisco Veterans Affairs Medical Center

Abstract

Objective—Peripheral artery disease (PAD) is a chronic condition characterized by inflammation. Emerging literature suggests that circulating exosomes and their microRNA (miRNA) contents may influence atherosclerosis and vascular remodeling. We hypothesize that circulating exosomes in patients with PAD directly modulate vascular cell phenotype and contain proinflammatory miRNAs.

Methods—Exosomes (particle size, 30–150 nm) were isolated from plasma of healthy individuals (n = 6), patients with mild PAD (mPAD; median Rutherford class, 2.5; n = 6), and patients with severe PAD (sPAD; median Rutherford class, 4; n = 5). Exosome identity, size, and concentration were determined by Western blot and nanoparticle tracking analysis. Human vascular smooth muscle cell (VSMC) and endothelial cell (EC) migration was assessed by a standard wound closure assay after exposure to exosome preparations. Monocyte-derived macrophages isolated from healthy volunteers were exposed to exosome preparations, and targeted gene expression was analyzed using quantitative polymerase chain reaction. Exosome miRNA cargos were isolated, and a panel of defined, vascular-active miRNAs was assessed by quantitative polymerase chain reaction.

Correspondence: Michael Conte, MD, Department of Surgery, University of California, San Francisco, 400 Parnassus Ave, Ste 501, San Francisco, CA 94143 (michael.conte2@ucsf.edu).

Results—There was no difference in overall exosome particle concentration or size between the three groups (one-way analysis of variance [ANOVA], $P > .05$). Compared with exosomes from healthy individuals, exosomes from mPAD and sPAD patients increased VSMC migration (1.0 ± 0.09-fold vs 1.5 ± 0.09-fold vs 2.0 ± 0.12-fold wound closure; ANOVA, $P < .0001$) and inhibited EC migration (1.8 ± 0.07-fold vs 1.5 ± 0.04-fold vs 1.3 ± 0.02-fold wound closure; ANOVA, $P < .01$) in a stepwise fashion. Exosomes also induced changes in monocyte-derived macrophage gene expression that did not appear PAD specific. Hierarchical analysis of exosome miRNA revealed distinct clustering of vascular-active miRNAs between the three groups. Several miRNAs that promote inflammatory pathways in vascular cells were expressed at higher levels in exosomes from sPAD patients.

Conclusions—Circulating exosomes from individuals with PAD exert in vitro functional effects on VSMCs and ECs that may promote adverse vessel remodeling. Exosomes from healthy individuals, mPAD patients, and sPAD patients contain distinct signatures of immune-regulatory miRNA. Together these data suggest that the proinflammatory cargo of circulating exosomes correlates with atherosclerosis severity in PAD patients and could influence vascular injury and repair. (JVS: Vascular Science 2020;1:28–41.)

Clinical Relevance—Exosomes and their cargo have been implicated in several vascular remodeling processes including atherosclerosis, angiogenesis, and neointimal hyperplasia. In this study, we demonstrate that circulating exosomes from individuals with peripheral artery disease exert in vitro effects on vascular cells that may adversely affect vessel remodeling. Moreover, these exosomes contain elevated levels of vascular-active microRNA. Our results suggest that exosomes may serve as both biomarkers and effectors of vascular disease in patients with peripheral artery disease and motivate further investigation into the role of exosomes and their contents in aberrant remodeling in vascular diseases.

Keywords

Intercellular communication is key to the process of vascular repair and remodeling. Recent research has shown that exosomes, 30- to 150-nm extracellular vesicles that contain protein, messenger RNA, and non-coding RNA including microRNA (miRNA), facilitate cell-cell communication by selectively transporting signaling molecules. Exosomes arise from the release of intraluminal vesicles when multivesicular bodies fuse with the cell plasma membrane. They have been implicated in a variety of vascular remodeling processes, including angiogenesis, atherosclerosis, and neointimal hyperplasia, as well as in pathologic changes in primary hypertension, pulmonary arterial hypertension, and aortic aneurysms.[1]

In atherosclerosis, levels of several miRNAs contained within exosomes have been shown to correlate with severity of coronary artery disease.[2] More broadly, in vivo and in vitro models have shown that a host of miRNAs modulate vascular remodeling through effects on vascular smooth muscle cells (VSMCs), endothelial cells (ECs), macrophages, and inflammation.[3–6] In addition, emerging research suggests that postsurgical changes in circulating exosome quantity and content may correlate with known biomarkers of disease.

For example, in patients undergoing coronary artery bypass grafting, plasma concentrations of exosomes and their cargo of several cardiac-related miRNAs (miR-1, miR-24, miR-133a, miR-133b) increased after surgery and correlated with cardiac troponin levels.[7]

We hypothesize that circulating exosomes in patients with peripheral artery disease (PAD) influence atherosclerosis progression, vascular repair, and remodeling. Moreover, we hypothesize that circulating exosomes from PAD patients will contain distinct profiles of miRNA that correlate with clinical PAD severity. Our results suggest that exosomes may serve as both biomarkers and effectors of vascular disease in patients with PAD.

METHODS

Study population and blood collection

This study was approved by the University of California, San Francisco (UCSF) Institutional Review Board (12–08642 and 15–17371). Healthy individuals and patients with PAD were enrolled from the vascular surgery clinic at UCSF. Healthy individuals were eligible between the ages of 20 and 65 years and excluded if they had C-reactive protein level >2.0 mg/L or regularly used aspirin or nonsteroidal anti-inflammatory drugs. All PAD patients had ankle-brachial index <0.9 or toe-brachial index <0.6. Potential patients were excluded if they had chronic liver, kidney, or other inflammatory disorders; were prescribed immunosuppressive medication; or had a recent (<30 days) history of major surgery or illness. Comorbidities of interest (coronary artery disease, hypertension, diabetes) were derived from review of the patient's electronic medical records. Plasma samples were obtained by single-time blood draw into Vacutainer tubes (Becton-Dickinson, Franklin Lakes, NJ) using ethylenediaminetetraacetic acid (1.8 mg/mL blood) as an anticoagulant. Blood samples were centrifuged at 2300 g for 15 minutes, after which plasma was aliquoted in cryovials and immediately stored at −80°C.

Exosome isolation

Exosomes were isolated from plasma using cushioned-density gradient ultracentrifugation as recently described.[8] Briefly, 800 μL of stored plasma was thawed, diluted in 39 mL of cold phosphate-buffered saline (PBS), transferred to an ultracentrifuge tube, underlaid with 2 mL of 60% iodixanol, and centrifuged at 100,000 g for 3 hours in a Beckman Ti 50.2 rotor. The bottom 2 mL of iodixanol and 1 mL of supernatant were aspirated and stored. Next, solutions containing 5%, 10%, and 20% iodixanol were prepared in a homogenization buffer containing 0.25 M sucrose, 1 mM ethylenediaminetetraacetic acid, and 10 mM Tris-HCL, pH 7.4. A step gradient was prepared by layering 3 mL of 20%, 10%, 5% (bottom to top), after which the ultracentrifuged iodixanol-supernatant concentrate was placed below the discontinuous gradient. The gradient was centrifuged at 100,000 g for 18 hours using a Beckman SW 40 Ti rotor, then 12 fractions of 1 mL were collected from the top of the tube for subsequent analysis.

Nanoparticle tracking analysis (NTA)

NTA was used to determine exosome concentration and size. Briefly, samples were diluted in PBS to a concentration of 10^8 to 10^9 nanoparticles per milliliter. Data were collected as

the average of three 1-minute-long videos with parameters of camera level 13 and detection threshold 3. All NTA experiments were performed on an LM14 NanoSight instrument (Malvern Pananalytical, Malvern, United Kingdom).

Western blot for exosome characterization

Exosome purity and protein contamination were determined by Western blot for exosome-specific proteins Flotillin-1 and CD9 and plasma protein stain Ponceau S. Briefly, Western blots were conducted by taking an aliquot of fractions 4 to 12 of the final density gradient; 37.5 μL of each fraction was mixed with 4 × Laemmli buffer containing 2-mercaptoethanol. The sample was boiled at 95°C for 5 minutes and resolved by sodium dodecyl sulfate-polyacrylamide gel electrophoresis on a 10% gel. The gel was transferred onto a polyvinylidene difluoride membrane using a standard tank protocol. The membrane was stained with 0.1% w/v Ponceau S to visualize total protein, followed by a 1-hour block in 5% nonfat milk. The membrane was probed with CD9 (Abcam, Cambridge, Mass) and Flotillin-1 (Cell Signaling Technology, Danvers, Mass) in 1% nonfat milk. The primary antibodies were used at a dilution of 1:500. The membrane was washed with 0.1% PBS-T detergent and probed with an anti-rabbit horseradish peroxidase antibody (1:1000 dilution; ThermoFisher Scientific, Waltham, Mass). Subsequently, the membrane was rewashed with 0.1% PBS-T and visualized using enhanced chemiluminescence on an ImageQuant LAS 4000 (GE Healthcare Life Sciences, Marlborough, Mass).

Vascular cell culture and wound closure assays

Primary cultures of human saphenous vein-derived VSMCs and ECs were prepared from discarded vein segments under a UCSF Institutional Review Board-approved protocol. VSMCs were cultured in 24-well plates to 100% confluence in low-glucose Dulbecco modified Eagle medium (ThermoFisher) supplemented with 10% fetal bovine serum (FBS). ECs were cultured in 24-well plates to 100% confluence in EC media containing Media 199 with Earle's balanced salt solution (HyClone) supplemented with 10% FBS, penicillin-streptomycin-amphotericin B (1760; Lonza, Bend, Ore), endothelial cell growth supplement (BD Biosciences, San Jose, Calif), and heparin (17.5 units/mL; Sigma-Aldrich, St. Louis, Mo).

To assess VSMC migration, a longitudinal scratch was made in the confluent cell monolayer with the tip of a 200-μL pipette, after which the plate was washed twice with warm PBS with calcium and magnesium and replaced with serum-free media. Cells were treated with iodixanol vehicle (negative control), platelet-derived growth factor (10 ng/mL, positive control), or ~10^{10} nanoparticles per milliliter. Images of the wound were taken at baseline and after 16 hours using a phase-contrast inverted microscope (Keyence Corp, Itasca, Ill). Wound closure was calculated as follows: (wound area at baseline–wound area at 16 hours)/ (wound area at baseline) and normalized to the negative control. To assess EC migration, a similar scratch procedure was carried out, after which the plates were washed and replaced with EC medium containing either 10% or 1% FBS (negative control). To the 10% FBS EC medium wells, either iodixanol vehicle alone (positive control) or ~10^{10} nanoparticles per milliliter were added to each well, and images were taken at baseline and after 12 hours. Wound closure analysis was performed as described before.

Human monocyte-derived macrophage (MDM) gene expression

Monocytes were isolated from the whole blood of healthy volunteers (UCSF Institutional Review Board-approved protocol 16–20174) using density gradient centrifugation and differentiated into macrophages in Roswell Park Memorial Institute (RPMI) medium (ThermoFisher) supplemented with 5% FBS and granulocyte-macrophage colony-stimulating factor (10 ng/mL) for 7 days. After differentiation, the medium was replaced and macrophages were treated with vehicle or 10^{10} nanoparticles per milliliter for 24 hours, at which point the cells were lysed with buffer RLT (Qiagen, Hilden, Germany) containing 1% β-mercaptoethanol. Total RNA was isolated using an RNeasy Micro Kit (Qiagen) and quantified using a NanoDrop 2000 (ThermoFisher). Complementary DNA (cDNA) was made by reverse transcription-polymerase chain reaction (PCR) using 1 μg of RNA. Real-time PCR was performed using a Fast SYBR Green kit (Life Technologies, Carlsbad, Calif) to assay for expression of tumor necrosis factor α (TNF-α), monocyte chemoattractant protein 1 (MCP-1), C-X-C motif chemokine 10 (CXCL10), interleukin 10 (IL-10), chemokine (C-C motif) ligand 17 (CCL17), and mannose receptor C-type 1 (MRC1) genes (see Supplementary Table, for primer sequences). Data were normalized to two housekeeping genes, hypoxanthine-guanine phosphoribosyltransferase and ubiquitin C, and then to healthy individuals using the $2^{-\Delta \Delta Ct}$ method.

Extraction of miRNA and quantitative real-time PCR

Exosomes were lysed using QIAzol lysis buffer (Qiagen). Total RNA was extracted from ~1 to 2×10^{12} exosomes using the miRNeasy kit (Qiagen) per the manufacturer's protocol and quantified using the Quant-iT RiboGreen RNA Assay kit (ThermoFisher). Before cDNA synthesis, synthetic RNA spike-in UniSp6 was added to each sample for normalization. Equal amounts of RNA from each sample were converted to cDNA using the miRCURY LNA Universal RT microRNA PCR kit (Qiagen). Quantitative real-time PCR was performed using the miRCURY LNA SYBR Green PCR Kit (Qiagen) on the QuantStudio 7 Flex Real-Time PCR System (Applied Biosystems, Foster City, Calif). The expression of miR-21, miR-23b, miR-122, miR-126, miR-143, miR-145, miR-146a, miR-146b, miR-155, miR-181b, miR-195, miR-208a, miR-219, miR-221, miR222, and miR-1202 (Qiagen; see Supplementary Table, for primer sequences) was normalized to RNA spike-in UniSp6.

Statistical analysis

Statistical analysis for migration assays and macrophage gene expression was performed with GraphPad Prism 7 (GraphPad Software Inc, La Jolla, Calif) using one-way analysis of variance with post hoc Tukey multiple comparison test and unpaired Student *t*-tests with Bonferroni correction as appropriate. Hierarchical clustering of miRNA PCR data was performed using MetaboAnalyst 4.0.[9] All data values are reported as mean ± standard error unless otherwise denoted. P value <.05 was considered statistically significant.

RESULTS

Description of study cohort

The study population comprised three separate groups: healthy individuals (n = 6), patients with mild PAD (mPAD; n = 6), and patients with severe PAD (sPAD; n = 5). Mild PAD was defined clinically as Rutherford stage 2 or 3 with intermittent, nondisabling claudication considered to be clinically stable and not requiring intervention. Severe PAD was defined as Rutherford stage 3 to stage 5, with clinical disease severe enough to require lower extremity bypass grafting. Compared with mPAD patients, sPAD patients had higher median Rutherford stage (2.5 vs 4), were more likely to be diabetic (33% vs 80%), and were less likely to take aspirin (100% vs 80%) or a statin (83% vs 60%; Table). There was no difference in mean ankle-brachial index, burden of coronary artery disease, hypertension, hyperlipidemia, or pack-year smoking history between the mPAD and sPAD groups (Table).

Exosome size and plasma concentration are not changed by presence or clinical severity of PAD

To investigate differences in the size and concentration of exosomes derived from plasma of healthy individuals, mPAD patients, and sPAD patients, exosomes were first isolated from plasma using cushioned-density gradient ultracentrifugation. To characterize exosome purity, individual fractions of the density gradient were probed with antibodies to known exosome-enriched proteins Flotillin-1 and CD9 as well as for plasma protein using Ponceau S stain (Fig 1, A). Analysis with NTA showed that isolated nanoparticles were 30 to 150 nm (Fig 1, B), consistent with standard size definitions for exosomes, and free of contamination from larger extracellular vesicles such as microvesicles. Fraction 9 was chosen for downstream assays because of high concentration of Flotillin-1- and CD9-positive particles without contamination from plasma protein. Characterization of exosome particle concentration (Fig 1, C) and size (Fig 1, D) by NTA demonstrated no significant difference across the three groups (analysis of variance, $P > .05$).

Exosomes from PAD patients promote VSMC migration and inhibit EC migration in a PAD severity-dependent manner

To investigate the effects of exosomes from PAD patients on vascular cell migration, we performed wound closure assays using monolayers of human primary saphenous vein VSMCs and ECs treated with exosomes from healthy individuals, mPAD patients, and sPAD patients. Compared with healthy exosomes, mPAD and sPAD exosomes significantly increased VSMC migration in the wound assay, with sPAD exosomes increasing migration more than mPAD exosomes (1.0 ± 0.2-fold [healthy] vs 1.5 ± 0.2-fold [mPAD] vs 2.0 ± 0.3-fold [sPAD] compared with vehicle [negative control]; $P < .05$ between all groups; Fig 2, A and B). Conversely, compared with healthy exosomes, mPAD and sPAD exosomes significantly inhibited EC migration, with sPAD exosomes inhibiting EC migration more than mPAD exosomes (1.8 ± 0.1-fold [healthy] vs 1.5 ± 0.1-fold [mPAD] vs 1.4 ± 0.05-fold [sPAD] compared with negative control; $P < .05$ between all groups).

Treatment with healthy exosomes did not significantly alter EC migration compared with treatment with 10% FBS with vehicle alone (positive control; 1.8 ± 0.2-fold [vehicle] vs 1.8

± 0.1-fold [healthy]; $P > .05$; Fig 2, C and D). Analysis of VSMC and EC migration based on whether exosomes were derived from nondiabetic and diabetic patients or nonsmokers, former smokers, and current smokers did not reveal any significant differences (Supplementary Fig 1).

Exosomes alter MDM gene expression

To investigate the effects of exosomes on macrophage phenotype, human MDMs from nonautologous healthy donors were treated with vehicle or exosomes from healthy individuals, mPAD patients, and sPAD patients. We then assayed for gene expression of M1-related TNF-α, MCP-1, and CXCL10 and M2-related IL-10, CCL17, and MRC1. Compared with vehicle, exosomes from both healthy individuals and mPAD patients significantly increased TNF-α expression, but sPAD exosomes had more variable effects (2.5 ± 0.6-fold vs 1.8 ± 0.6-fold vs 3.2 ± 2.3-fold change compared with vehicle; Fig 3, A). A similar pattern was observed in the expression of MCP-1 (2.7 ± 0.7 vs 2.4 ± 0.5 vs 1.6 ± 0.8 compared with vehicle; Fig 3, B). There were no significant changes in MDM expression of CXCL10, IL-10, CCL17, or MRC1 between the three groups compared with vehicle (Fig 3, C–F).

Hierarchical analysis of exosome miRNA reveals distinct clustering based on PAD severity

To investigate differences in the molecular content of healthy, mPAD, and sPAD exosomes that may explain their observed effects on vascular cell migration, we assayed exosomes for 15 different miRNAs known to alter vascular cell phenotype or function. The miRNAs with cycle threshold values above 35 were excluded from subsequent analysis, leaving miR-21, miR-92a, miR-126, miR-143, miR-146a, miR-146b, miR-181b, miR-221, and miR-1202 (control miR) for analysis. Hierarchical cluster analysis revealed distinct clustering of sPAD patients' exosome miRNA compared with healthy or mPAD exosome miRNA (Fig 4, A). Of note, miR-21, miR-92a, miR-126, miR-143, miR-181b, and miR-221 were elevated in the exosomes from sPAD patients compared with those isolated from healthy individuals or mPAD patients. This finding was recapitulated in a volcano plot analysis of miRNA from exosomes of mPAD vs sPAD patients, which revealed significantly elevated levels of miR-21, miR-92a, miR-126, and miR-143 in sPAD exosomes (Fig 4, B). Principal component analysis also revealed differences in the overall miRNA content between the mPAD and sPAD groups (Supplementary Fig 2).

DISCUSSION

The results of this study suggest that circulating exosomes are capable of directly influencing vascular cell phenotype and processes that are central to vascular disease, repair, and remodeling. Impaired reendothelialization and augmented VSMC migration both tend to promote neointimal hyperplasia, central to both atheroprogression and restenosis after vascular intervention. Using surrogate in vitro assays, this study shows that plasma-derived exosomes from PAD patients increase VSMC migration and decrease EC migration in a manner that correlates with clinical disease severity.

Circulating exosomes also influenced MDM gene transcription, although a PAD-specific pattern was not demonstrated in this pilot study. The miRNA cargo is an established signaling mechanism by which exosomes exert paracrine and remote effects on cells. We found that exosomes from patients with different clinical severities of PAD clustered into distinct groups based on the content of several established vascular-active miRNAs. Together, these results suggest that exosome-derived contents (eg, miRNA) may influence vascular inflammation, repair, and remodeling processes that underlie disease progression and treatment responses in PAD.

In this investigation, we found that circulating exosomes from healthy individuals did not alter VSMC migration, whereas those from PAD patients promoted VSMC migration in a wound closure assay. Indeed, previous literature has linked burden of atherosclerotic disease with the cellular effects of exosomes.[10] Extracellular vesicles derived from macrophage foam cells were shown to increase VSMC migration by regulating actin cytoskeleton and focal adhesion pathways as well as to alter VSMC surface integrin expression.[11] Moreover, exosome-dependent transfer of angiotensin-converting enzyme from adventitial fibroblasts to VSMCs was shown to induce significant VSMC migration in a rat model of hypertension.[12] Our findings build on these results by demonstrating a correlation between peripheral atherosclerosis severity and circulating exosome-induced VSMC migration.

Our study also demonstrated that exosomes from PAD patients inhibited EC migration, a key function in the re-endothelialization that occurs after vascular injury. Other studies have demonstrated that exosome-delivered miRNAs have proatherogenic effects on ECs. For example, miR-155 transferred to ECs by VSMC-derived exosomes inhibited EC migration and disrupted endothelial tight junctions, increasing vascular permeability and enhancing atherosclerotic progression.[13] Of note, miR-155 was not reliably detected in the exosomes isolated in our study, nor was the cellular source of these plasma exosomes characterized. Although we did not examine EC adhesion molecule or proinflammatory gene expression, previous reports reveal that exosomes derived from monocytes and macrophages exposed to inflammatory conditions increase EC intercellular adhesion molecule 1 protein levels and expression of interleukin 6 and CCL2 genes.[14,15] Conversely, exosomes derived from endothelial progenitor cells have been shown to confer vascular-protective effects on ECs. Endothelial progenitor cell-derived exosomes have been shown to accelerate re-endothelialization and to promote diabetic wound healing by promoting angiogenesis.[16,17] Studies examining specific cell-derived exosomes vs circulating exosomes cannot be directly compared but collectively demonstrate the relevance of exosome signaling on inflammation, repair, and remodeling in the vasculature. Our data lend complementary evidence in this regard.

The miRNAs assayed in this study were intentionally selected because of their reported effects in vascular cell remodeling. Hierarchical cluster and volcano plot analysis revealed relatively elevated levels of miR-181b, miR-21, miR-92a, miR-126, and miR-221 in the exosomes of sPAD patients, all of which have been shown to confer potentially important effects on vessel remodeling. The miR-181b activates canonical proliferation and inflammation protein families in VSMCs, including phosphatidylinositol 3-kinase, mitogen-activated protein kinase, and nuclear factor kB.[18,19] Moreover, miR-181b has been shown to

promote VSMC migration in a serum response factor-dependent manner.[20] Interestingly, one conflicting report by Sun et al[21] demonstrated that patients with coronary artery disease have lower circulating levels of miR-181b. They also found that systemic delivery of an miR-181b mimic in ApoE$^{-/-}$ mice suppressed nuclear factor κB activation, inhibited atherosclerotic lesion formation, and blunted proinflammatory gene expression in the aortic wall.[21] Multiple reports have shown that miR-21 is elevated in animal models of in-stent restenosis and vein bypass grafting and that miR-21 knockout or application of locked nucleic acid anti-miR-21 effectively suppresses neointimal hyperplasia.[22–24] Recent investigations have revealed that miR-92a alters both VSMC and EC migration. Production of miR-92a is activated by Rho-associated coiled-coil-forming kinase and myosin light chain kinase, subsequently leading to enhanced VSMC migration and proliferation through a platelet-derived growth factor subunit BB-mediated mechanism.[25] Furthermore, miR-92a has been shown to inhibit EC proliferation and migration in vitro, and systemic inhibition of miR-92a accelerated reendothelialization and inhibited neointimal hyperplasia of mouse femoral arteries damaged by wire injury.[26] Mechanistically, miR-221 accelerates neointimal hyperplasia by suppressing the messenger RNA encoding the cyclin-dependent kinase p27^{Kip1} and has been shown to promote both VSMC migration and proliferation while simultaneously inhibiting the same processes in ECs.[27,28] In addition, in a mouse model of diabetes, miR-221 was found to be elevated in an extracellular signal-regulated protein kinase-dependent manner, and miR-221 inhibition attenuated neointimal hyperplasia after femoral artery wire injury.[29] Whereas our study found elevated levels of miR-126 in exosomes from sPAD patients, many studies have revealed a broadly atheroprotective and antiproliferative role for miR-126.[30–32] Our findings motivate continued investigation into the miRNA-dependent mechanisms by which circulating exosomes in patients with vascular disease may alter VSMC and EC phenotype and influence in vivo responses.

Macrophages that participate in the inflammatory response can broadly be classified as M1 (proinflammatory) or M2 (proresolving). M1 macrophages secrete proinflammatory cytokines including interleukin 1β and TNF-α and are functionally characterized by the ability to enhance endocytic capacity and to kill intracellular pathogens.[33] M2 macrophages primarily function to clear debris from the inflammatory milieu and significantly lower levels of proinflammatory cytokines.[33] Interestingly, in this study, treatment of human MDMs with exosomes from healthy individuals, mPAD patients, and sPAD patients led to a generalized polarization toward the M1 phenotype with trends in upregulation of TNF-α and MCP-1 after exposure to exosomes from all three groups. No clear effect on M2 polarization was observed. Other studies have found that exosomes alter macrophage polarization in models of coronary ischemia-reperfusion injury, diabetic wound healing, and atherosclerosis.[34–36] The definitions of M1 and M2 macrophages and their characteristic markers, particularly in humans, are in flux and the subject of extensive research.[37,38] Further studies are needed to characterize the effects of circulating exosomes in patients with atherosclerosis on acute and chronic vascular inflammation.

This pilot study is limited by its descriptive nature. Given the multitude of mechanisms described by which circulating exosomes may alter VSMC and EC phenotype and function, the overall effect is almost certainly a complex integration of signaling pathways. In addition, exosomes are known to carry a wide variety of proteins, lipids, and other

noncoding RNA species not measured here that may contribute to effects on the vessel wall. Future studies should focus on defining disease- and clinical stage-specific molecular signatures within exosomes, and investigation into their role in influencing vascular repair and remodeling (eg, in animal models) will be a key step in the translational research process. Moreover, investigation into the role of circulating exosomes in additional key processes in the development of atherosclerotic lesions, including endothelial dysfunction, monocyte migration, macrophage phenotype, matrix remodeling, and plaque stability, should be pursued. Further studies into the utility of circulating exosomes as diagnostic or prognostic biomarkers in PAD, as is being undertaken in other disease processes, are warranted on the basis of the findings of this study.[39–42] Future work should also attempt to identify the cellular origin of the exosomes, and various methods involving both surface proteomics and comparing exosome content to originating cell content have been explored. [43,44] Therapeutic applications of exosomes are also being avidly pursued, and these studies highlight the potential heterogeneity of exosome sources and preparations that will need to be better characterized to advance such concepts.

CONCLUSIONS

Plasma-derived exosomes from healthy individuals and PAD patients contain distinct signatures of immune-regulatory miRNA. In addition, circulating exosomes have in vitro functional effects on VSMCs and ECs that may have an impact on vessel remodeling. Together these data suggest that the proinflammatory cargo of circulating exosomes correlates with clinical disease severity in PAD patients and may influence treatment responses.

Supplementary Material

Refer to Web version on PubMed Central for supplementary material.

Acknowledgments

REFERENCES

1. Su SA, Xie Y, Fu Z, Wang Y, Wang JA, Xiang M. Emerging role of exosome-mediated intercellular communication in vascular remodeling. Oncotarget 2017;8:25700–12. [PubMed: 28147325]

2. Boulanger CM, Loyer X, Rautou PE, Amabile N. Extracellular vesicles in coronary artery disease. Nat Rev Cardiol 2017;14: 259–72. [PubMed: 28150804]

3. Polimeni A, De Rosa S, Indolfi C. Vascular miRNAs after balloon angioplasty. Trends Cardiovasc Med 2013;23:9–14. [PubMed: 23312133]

4. Gareri C, Rosa SD, Indolfi C. MicroRNAs for restenosis and thrombosis after vascular injury. Circ Res 2016;118:1170–84. [PubMed: 27034278]

5. Essandoh K, Li Y, Huo J, Fan GC. miRNA-Mediated macrophage polarization and its potential role in the regulation of inflammatory response. Shock 2016;46:122–31. [PubMed: 26954942]

6. Recchiuti A, Serhan CN. Pro-resolving lipid mediators (SPMs) and their actions in regulating miRNA in novel resolution circuits in inflammation. Front Immunol 2012;3:298. [PubMed: 23093949]

7. Emanueli C, Shearn AI, Laftah A, Fiorentino F, Reeves BC, Beltrami C, et al. Coronary artery-bypass-graft surgery increases the plasma concentration of exosomes carrying a cargo of cardiac microRNAs: an example of exosome trafficking out of the human heart with potential for cardiac biomarker discovery. PLoS One 2016;11:e0154274. [PubMed: 27128471]

8. Duong P, Chung A, Bouchareychas L, Raffai RL. Cushioned-density gradient ultracentrifugation (C-DGUC) improves the isolation efficiency of extracellular vesicles. PLoS One 2019;14: e0215324. [PubMed: 30973950]

9. Chong J, Soufan O, Li C, Caraus I, Li S, Bourque G, et al. MetaboAnalyst 4.0: towards more transparent and integrative metabolomics analysis. Nucleic Acids Res 2018;46: W486–94. [PubMed: 29762782]

10. Wang Y, Xie Y, Zhang A, Wang M, Fang Z, Zhang J. Exosomes: an emerging factor in atherosclerosis. Biomed Pharmacother 2019;115:108951. [PubMed: 31078042]

11. Niu C, Wang X, Zhao M, Cai T, Liu P, Li J, et al. Macrophage foam cell-derived extracellular vesicles promote vascular smooth muscle cell migration and adhesion. J Am Heart Assoc 2016;5:e004099. [PubMed: 27792649]

12. Tong Y, Ye C, Ren XS, Qiu Y, Zang YH, Xiong XQ, et al. Exosome-mediated transfer of ACE (angiotensin-converting enzyme) from adventitial fibroblasts of spontaneously hypertensive rats promotes vascular smooth muscle cell migration. Hypertension 2018;72:881–8. [PubMed: 30354715]

13. Zheng B, Yin W, Suzuki T, Zhang X, Zhang Y, Song L, et al. Exosome-mediated miR-155 transfer from smooth muscle cells to endothelial cells induces endothelial injury and promotes atherosclerosis. Mol Ther 2017;25:1279–94. [PubMed: 28408180]

14. Tang N, Sun B, Gupta A, Rempel H, Pulliam L. Monocyte exosomes induce adhesion molecules and cytokines via activation of NF-κB in endothelial cells. FASEB J 2016;30: 3097–106. [PubMed: 27226520]

15. Osada-Oka M, Shiota M, Izumi Y, Nishiyama M, Tanaka M, Yamaguchi T, et al. Macrophage-derived exosomes induce inflammatory factors in endothelial cells under hypertensive conditions. Hypertens Res 2017;40:353–60. [PubMed: 27881852]

16. Zhang J, Chen C, Hu B, Niu X, Liu X, Zhang G, et al. Exosomes derived from human endothelial progenitor cells accelerate cutaneous wound healing by promoting angiogenesis through Erk½ signaling. Int J Biol Sci 2016;12:1472–87. [PubMed: 27994512]

17. Li X, Chen C, Wei L, Li Q, Niu X, Xu Y, et al. Exosomes derived from endothelial progenitor cells attenuate vascular repair and accelerate re-endothelialization by enhancing endothelial function. Cytotherapy 2016;18:253–62. [PubMed: 26794715]

18. Pierdomenico AM, Recchiuti A, Simiele F, Codagnone M, Mari VC, Davì G, et al. MicroRNA-181b regulates ALX/FPR2 receptor expression and proresolution signaling in human macrophages. J Biol Chem 2015;290:3592–600. [PubMed: 25505240]

19. Li TJ, Chen YL, Gua CJ, Xue SJ, Ma SM, Li XD. MicroRNA 181b promotes vascular smooth muscle cells proliferation through activation of PI3K and MAPK pathways. Int J Clin Exp Pathol 2015;8:10375–84. [PubMed: 26617745]

20. Wei X, Hou X, Li J, Liu Y. miRNA-181a/b regulates phenotypes of vessel smooth muscle cells through serum response factor. DNA Cell Biol 2017;36:127–35. [PubMed: 27911586]

21. Sun X, He S, Wara AK, Icli B, Shvartz E, Tesmenitsky Y, et al. Systemic delivery of microRNA-181b inhibits nuclear factor-κB activation, vascular inflammation, and atherosclerosis in apolipoprotein E-deficient mice. Circ Res 2014;114:32–40. [PubMed: 24084690]

22. McDonald RA, Halliday CA, Miller AM, Diver LA, Dakin RS, Montgomery J, et al. Reducing in-stent restenosis. J Am Coll Cardiol 2015;65:2314–27. [PubMed: 26022821]

23. McDonald RA, White KM, Wu J, Cooley BC, Robertson KE, Halliday CA, et al. miRNA-21 is dysregulated in response to vein grafting in multiple models and genetic ablation in mice attenuates neointima formation. Eur Heart J 2013;34:1636–43. [PubMed: 23530023]

24. Wang D, Deuse T, Stubbendorff M, Chernogubova E, Erben RG, Eken SM, et al. Local microRNA modulation using a novel anti-miR-21-eluting stent effectively prevents experimental in-stent restenosis. Arterioscler Thromb Vasc Biol 2015;35:1945–53. [PubMed: 26183619]

25. Wang J, Zhang C, Li C, Zhao D, Li S, Ma L, et al. MicroRNA-92a promotes vascular smooth muscle cell proliferation and migration through the ROCK/MLCK signalling pathway. J Cell Mol Med 2019;23:3696–710. [PubMed: 30907506]

26. Daniel JM, Penzkofer D, Teske R, Dutzmann J, Koch A, Bielenberg W, et al. Inhibition of miR-92a improves reendothelialization and prevents neointima formation following vascular injury. Cardiovasc Res 2014;103:564–72. [PubMed: 25020912]

27. Liu X, Cheng Y, Zhang S, Lin Y, Yang J, Zhang C. A necessary role of miR-221 and miR-222 in vascular smooth muscle cell proliferation and neointimal hyperplasia. Circ Res 2009;104: 476–87. [PubMed: 19150885]

28. Liu X, Cheng Y, Yang J, Xu L, Zhang C. Cell-specific effects of miR-22½22 in vessels: molecular mechanism and therapeutic application. J Mol Cell Cardiol 2012;52:245–55. [PubMed: 22138289]

29. Lightell DJ, Moss SC, Woods TC. Upregulation of miR-221 and −222 in response to increased extracellular signal-regulated kinases ½ activity exacerbates neointimal hyperplasia in diabetes mellitus. Atherosclerosis 2018;269:71–8. [PubMed: 29276985]

30. Harris TA, Yamakuchi M, Ferlito M, Mendell JT, Lowenstein CJ. MicroRNA-126 regulates endothelial expression of vascular cell adhesion molecule 1. Proc Natl Acad Sci U S A 2008;105:1516–21. [PubMed: 18227515]

31. Jansen F, Stumpf T, Proebsting S, Franklin BS, Wenzel D, Pfeifer P, et al. Intercellular transfer of miR-126–3p by endothelial microparticles reduces vascular smooth muscle cell proliferation and limits neointima formation by inhibiting LRP6. J Mol Cell Cardiol 2017;104:43–52. [PubMed: 28143713]

32. Qu Q, Bing W, Meng X, Xi J, Bai X, Liu Q, et al. Upregulation of miR-126–3p promotes human saphenous vein endothelial cell proliferation in vitro and prevents vein graft neointimal formation ex vivo and in vivo. Oncotarget 2017;8:106790–806. [PubMed: 29290989]

33. Martinez FO, Sica A, Mantovani A, Locati M. Macrophage activation and polarization. Front Biosci 2008;13:453–61. [PubMed: 17981560]

34. de Couto G, Gallet R, Cambier L, Jaghatspanyan E, Makkar N, Dawkins JF, et al. Exosomal microRNA transfer into macrophages mediates cellular postconditioning. Circulation 2017;136:200–14. [PubMed: 28411247]

35. Dalirfardouei R, Jamialahmadi K, Jafarian AH, Mahdipour E. Promising effects of exosomes isolated from menstrual blood-derived mesenchymal stem cell on wound-healing process in diabetic mouse model. J Tissue Eng Regen Med 2019;13:555–68. [PubMed: 30656863]

36. Xie Z, Wang X, Liu X, Du H, Sun C, Shao X, et al. Adipose-derived exosomes exert proatherogenic effects by regulating macrophage foam cell formation and polarization. J Am Heart Assoc 2018;7:e007442. [PubMed: 29502100]

37. Murray PJ, Allen JE, Biswas SK, Fisher EA, Gilroy DW, Goerdt S, et al. Macrophage activation and polarization: nomenclature and experimental guidelines. Immunity 2014;41:14–20. [PubMed: 25035950]

38. Murray PJ. Macrophage polarization. Annu Rev Physiol 2017;79:541–66. [PubMed: 27813830]

39. Kennel PJ, Saha A, Maldonado DA, Givens R, Brunjes DL, Castillero E, et al. Serum exosomal protein profiling for the non-invasive detection of cardiac allograft rejection. J Heart Lung Transplant 2018;37:409–17. [PubMed: 28789823]

40. Street JM, Koritzinsky EH, Glispie DM, Star RA, Yuen PS. Urine exosomes: an emerging trove of biomarkers. Adv Clin Chem2017;78:103–22.

41. Bei Y, Yu P, Cretoiu D, Cretoiu SM, Xiao J. Exosomes-based biomarkers for the prognosis of cardiovascular diseases. Adv Exp Med Biol 2017;998:71–88. [PubMed: 28936733]

42. Jansen F, Li Q. Exosomes as diagnostic biomarkers in cardiovascular diseases. Adv Exp Med Biol 2017;998:61–70. [PubMed: 28936732]

43. Castillo J, Bernard V, San Lucas FA, Allenson K, Capello M, Kim DU, et al. Surfaceome profiling enables isolation of cancer-specific exosomal cargo in liquid biopsies from pancreatic cancer patients. Ann Oncol 2018;29:223–9. [PubMed: 29045505]

44. Wu D, Yan J, Shen X, Sun Y, Thulin M, Cai Y, et al. Profiling surface proteins on individual exosomes using a proximity barcoding assay. Nat Commun 2019;10:3854. [PubMed: 31451692]

## ARTICLE HIGHLIGHTS

Type of Research

Human study, in vitro study

Key Findings

Plasma-derived exosomes from patients with mild and severe peripheral artery disease (PAD) increased vascular smooth muscle cell migration and inhibited endothelial cell migration compared with exosomes from healthy individuals but did not alter expression of inflammation-related genes in monocyte-derived macrophages. There was distinct clustering of exosome vascular-active microRNA between the groups.

Take Home Message

Circulating exosomes from PAD patients contain elevated levels of proinflammatory microRNA cargo and alter in vitro migration of vascular smooth muscle cells and endothelial cells, suggesting that they may influence vascular injury and repair. Exosome effects correlate with atherosclerosis severity in PAD patients.
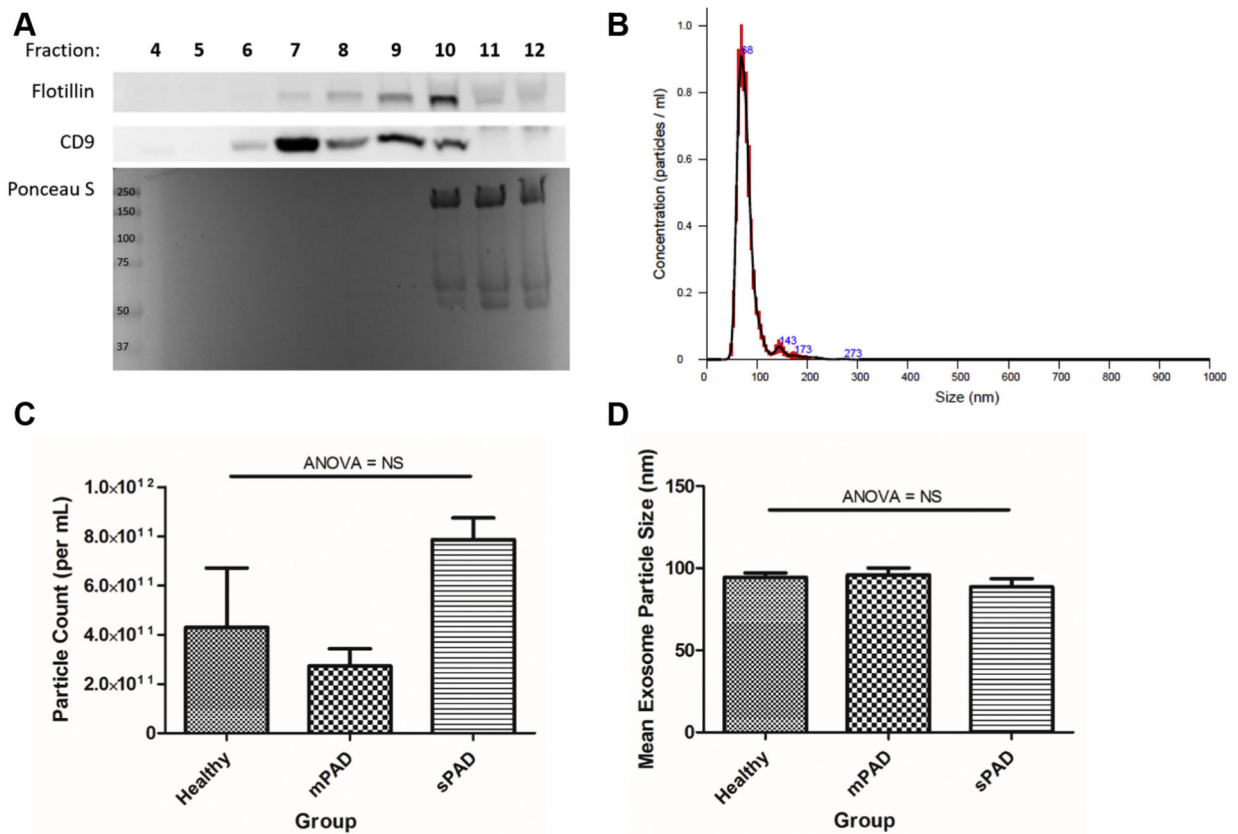
Fig 1.

Exosome isolation and characterization. Exosomes were isolated by cushioned density gradient ultracentrifugation. Representative Western blot for Flotillin-1, CD9, and plasma protein (Ponceau S) shows relative purity and contamination **(A)**. Exosome particles were found to be ~30 to 150 nm in size using a nanoparticle tracking analyzer **(B)**. There was no difference in overall exosome particle count **(C)** or size **(D)** between the three groups (one-way analysis of variance [*ANOVA*], $P > .05$). Data are reported as mean ± standard error of the mean, n = 5–6/group. *mPAD*, Mild peripheral artery disease; *NS*, not significant; *sPAD*, severe peripheral artery disease.
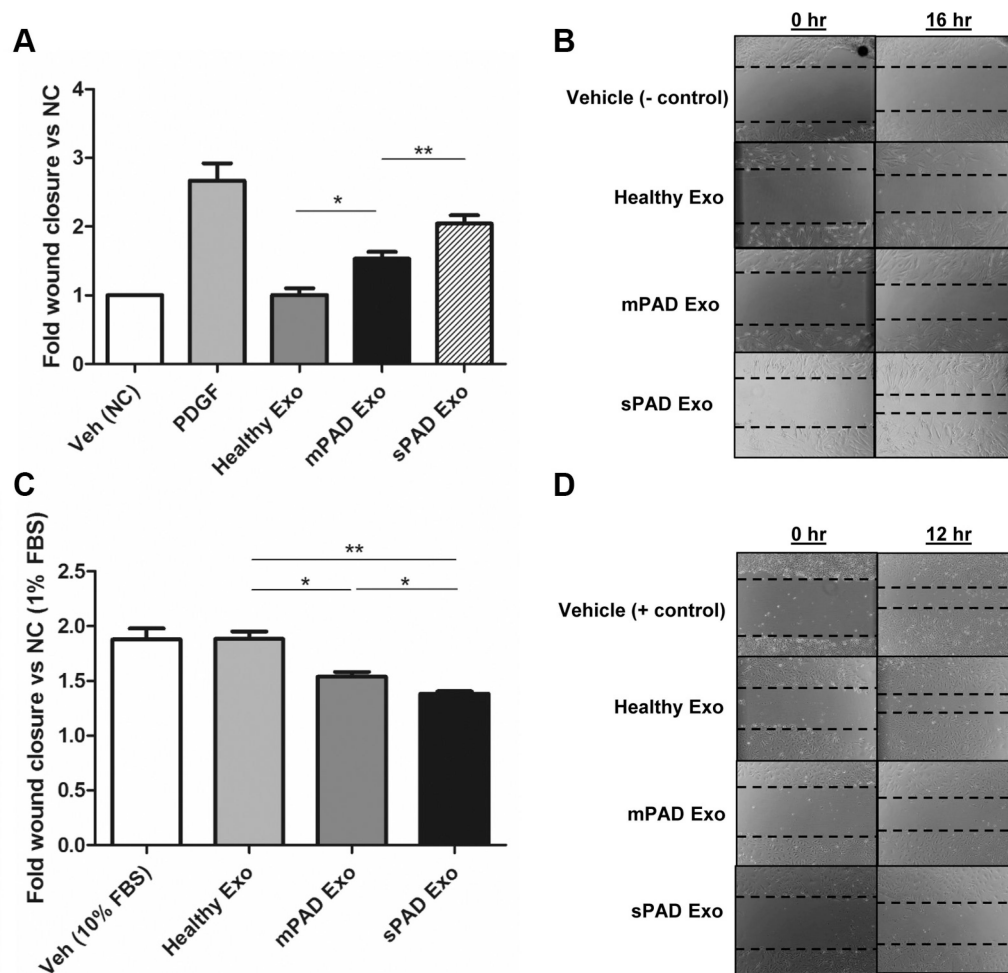
Fig 2.
Exosomes from peripheral artery disease (PAD) patients increase vascular smooth muscle cell (VSMC) migration and decrease endothelial cell (EC) migration. Fold change **(A)** and representative images **(B)** of VSMC migration in a wound closure assay when treated with vehicle (*Veh*; iodixanol, negative control [*NC*]), 10 nM platelet-derived growth factor (*PDGF*; positive control), and healthy, mild PAD (*mPAD*), or severe PAD (*sPAD*) exosomes (*Exo*) for 16 hours. The mPAD and sPAD exosomes significantly increase VSMC migration compared with vehicle and healthy exosomes. Fold change **(C)** and representative images **(D)** of endothelial cell (EC) migration in a wound closure assay when treated with vehicle (10% fetal bovine serum [*FBS*] medium + iodixanol) and healthy, mPAD, or sPAD exosomes for 12 hours compared with negative control (1% FBS media). The mPAD and sPAD exosomes significantly decrease EC migration compared with vehicle and healthy exosomes. Fold wound closure was calculated as (wound area t = 0 – wound area t = end time)/wound area t = 0, normalized to the negative control. Data are reported as mean ± standard error of the mean, n = 5–6/group. *$P < .05$, **$P < .005$ (one-way analysis of variance with Tukey post hoc test).
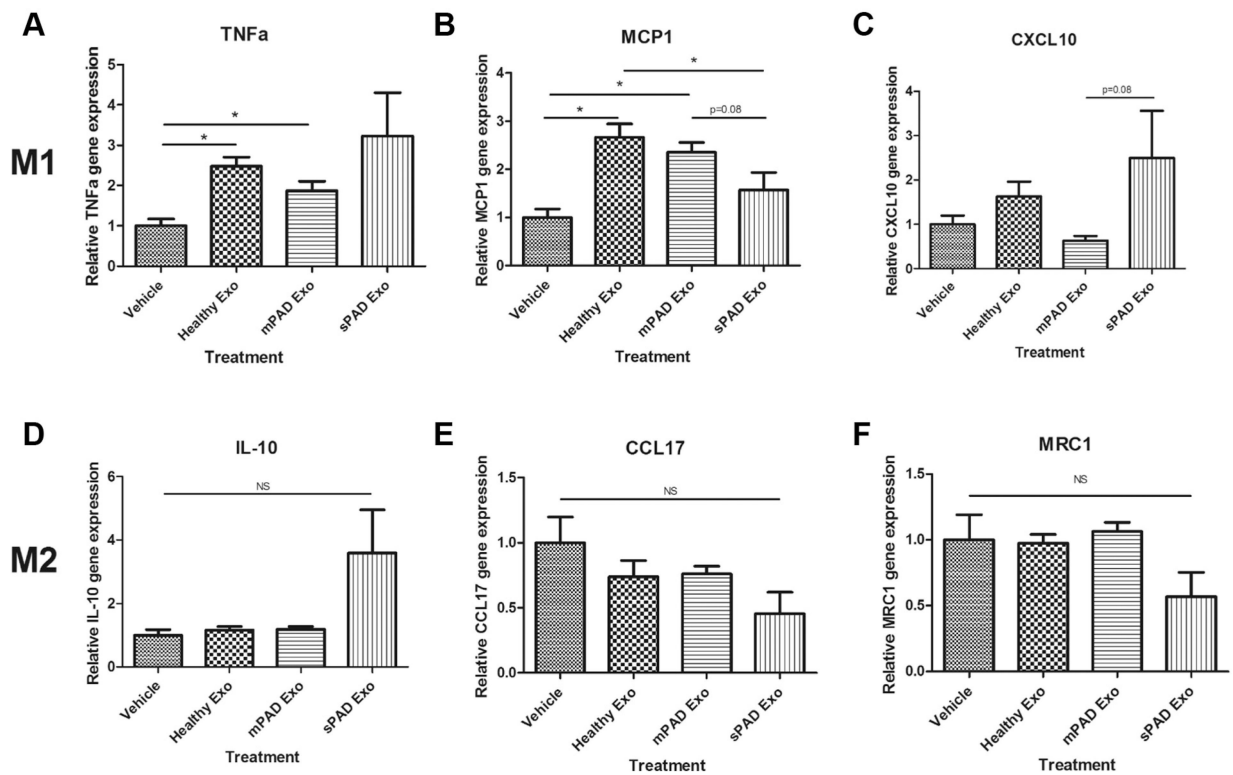
Fig 3.

Exosomes from peripheral artery disease (PAD) patients do not significantly alter M1-and M2-related gene expression in monocyte-derived macrophages (MDMs). Compared with vehicle or treatment with exosomes (*Exo*) from healthy individuals, exosomes from mild PAD (*mPAD*) or severe PAD (*sPAD*) patients did not significantly affect M1-related tumor necrosis factor α (*TNF-α*; **A**), monocyte chemoattractant protein 1 (*MCP-1*; **B**), or C-X-C motif chemokine 10 (*CXCL10*; **C**) or M2-related interleukin 10 (IL-10; **D**), chemokine (C-C motif) ligand 17 (*CCL17*; **E**), or mannose receptor C-type 1 (*MRC1*; **F**) expression, except where noted. Relative gene expression was calculated using the $2^{-\Delta Ct}$ method with normalization to two housekeeping genes, hypoxanthine-guanine phosphoribosyltransferase and ubiquitin C. Data are reported as mean ± standard error of the mean, n = 5–6/group. *P < .05 (one-way analysis of variance with Tukey post hoc test). *NS*, Not significant.

A

B
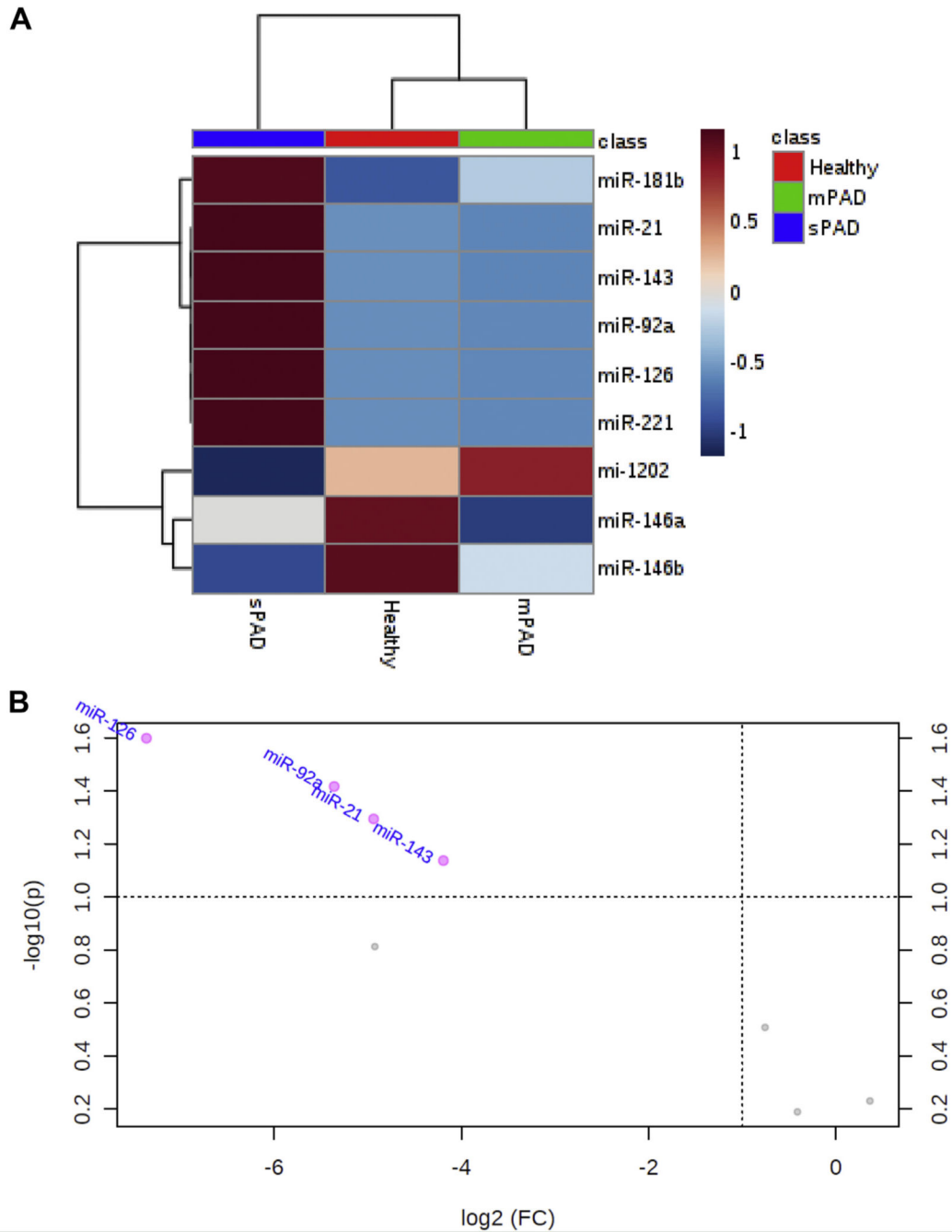
Fig 4.

Hierarchical cluster analysis and volcano plot reveal distinct clustering of exosome vascular-active microRNA (miRNA) based on severity of peripheral artery disease (PAD). After normalization to a spike-in control, quantitative polymerase chain reaction data from nine miRNAs with cycle threshold values <35 were used to perform a hierarchical cluster analysis **(A)**, which reveals clustering of patients with different severities of PAD based on their miRNA content. In addition, volcano plot analysis **(B)** shows significantly lower

expression of miR-21, miR-92a, miR-126, and miR-143 in mild PAD (*mPAD*) patients compared with severe PAD (*sPAD*) patients. *FC*, Fold change.

Table.

Patients' characteristics

Characteristic	Healthy (n = 6)	mPAD (n = 6)	sPAD (n =5)
Age, years	56.8 (54–62)	73.8 (72–76)	69 (68–82)
Male sex	2 (33.3)	4 (66.7)	4 (80)
Clinical measurements at baseline			
Creatinine concentration, mg/dL	0.84 (0.16)	1.14 (0.16)	1.00 (.30)
ABI	–	0.71 (0.45–0.80)	0.74 (0.57–0.79)
Rutherford stage	–	2.5 (2–3)	4 (3–5)
Medical history			
Coronary artery disease	0	1 (16.7)	1 (20)
Hypertension	0	6 (100.0)	5 (100)
Hyperlipidemia	0	6 (100.0)	5 (100)
Diabetes	0	2 (33.3)	4 (80)
Tobacco use			
Never	4 (66.7)	0 (0.0)	1 (20)
Current	0	1 (16.7)	1 (20)
Pack years smoked		30	50
Former	2 (33.3)	5 (83.3)	3 (60)
Pack-years smoked	4 (3.88–12)	35 (24–40)	60 (35–60)
Takes daily aspirin	0	6 (100.0)	4 (80)
Takes daily statin	0	5 (83.3)	3 (60)

ABI, Ankle-brachial index; *mPAD*, mild peripheral artery disease; *sPAD*, severe peripheral artery disease.

Categorical variables are presented as number (%). Continuous variables are presented as mean (standard deviation) or median (interquartile range).

Mild PAD is defined as ABI <0.9 with intermittent, nondisabling claudication, Rutherford stage 2 to 3. Severe PAD is defined as ABI <0.9 warranting lower extremity bypass grafting, Rutherford stage 3 to 5.